CONF-9509279--2

SAND95-1917C

final draft, 9/26/95

IMPACTS OF SEISMIC ACTIVITY ON LONG-TERM REPOSITORY PERFORMANCE AT YUCCA MOUNTAIN

John H. Gauthier
SPECTRA Research Institute
1613 University Blvd. NE
Albuquerque, NM 87102
(505) 848-0808

Michael L. Wilson
Sandia National Labs.
Mail Stop 1326
Albuquerque, NM 87185
(505) 848-0770

David J. Borns
Sandia National Labs.
Mail Stop 0750
Albuquerque, NM 87185
(505) 844-7333

Bill W. Arnold
Sandia National Labs.
Mail Stop 1326
Albuquerque, NM 87185
(505) 848-0894

ABSTRACT

Several effects of seismic activity on the release of radionuclides from a potential repository at Yucca Mountain are quantified. Future seismic events are predicted using data from the seismic hazard analysis conducted for the Exploratory Studies Facility (ESF). Phenomenological models are developed, including rockfall (thermal-mechanical and seismic) in unbackfilled emplacement drifts, container damage caused by fault displacement within the repository, and flow-path change caused by changes in strain. Using the composite-porosity flow model (relatively large-scale, regular percolation), seismic events show little effect on total-system releases; using the weeps flow model (episodic pulses of flow in locally saturated fractures), container damage and flow-path changes cause over an order of magnitude increase in releases. In separate calculations using more realistic representations of faulting, water-table rise caused by seismically induced changes in strain are seen to be higher than previously estimated by others, but not sufficient to reach a potential repository.

INTRODUCTION

Possible disruption to waste containers or transport pathways caused by tectonic events is an important consideration in analyzing the long-term performance of a potential repository system at Yucca Mountain, Nevada.[1–3] Although the Yucca Mountain block itself appears to be relatively stable in recent time, evidence of recent tectonic activity exists throughout the region.[4–7] Repository disturbance due to volcanic activity and its consequences have been modeled in previous total-system performance assessments (TSPAs) performed for Yucca Mountain.[3,8–11] This paper outlines work in progress to define models to describe and quantify the effect of future seismic activity on releases of radionuclides from a potential repository for high-level radioactive waste; some work in this area has already been done by other groups.[3,9]

In this analysis, we consider the potential impact of the following seismic effects on long-term repository performance: (1) rockfall, (2) fault displacement, (3) changes in flow patterns (flow in fractures only), and (4) changes in water-table elevation. Simple phenomenological models are used for the most part, with parameters defined by probability distributions selected to represent our uncertainty. (Structuring the problem in this manner allows us to study the sensitivity of the resulting releases to variations in the parameters.) Several effects are omitted because they are less certain to occur, are generally expected to produce less severe consequences, or are too difficult to model at this time. At the end of this paper, we discuss ways in which this analysis could be improved by additional data and analyses.

SEISMIC MODEL DEVELOPMENT

Much of the analysis herein is based on prediction of the timing and magnitude of future seismic events. The data used in this analysis come from several sources, but have been synthesized in the ESF seismic hazard analysis.[12] Data from this report are given primarily in the form of yearly probabilities of a given seismic acceleration and velocity (Figure 1). We sample events from the data as follows. For every year in the future (actually, we use 10-yr periods for efficiency), we randomly select a probability level. The distributions of possible accelerations and velocities at a given probability level are assumed to be normal, with mean and standard deviation estimated from Figure 1. We sample the specific acceleration and velocity at that probability level for that year from the appropriate normal distribution. All events below a threshold, randomly chosen between $0.2g$ and $0.5g$, are ignored. This threshold is based on empirical estimates of the ground acceleration necessary to produce more than minor damage to a tunnel.[13] The sampled accelerations are reduced 50% and the velocities are reduced 40% to account for attenuation at depth.[12] Specification of fault offset, length, and location, as well as changes of

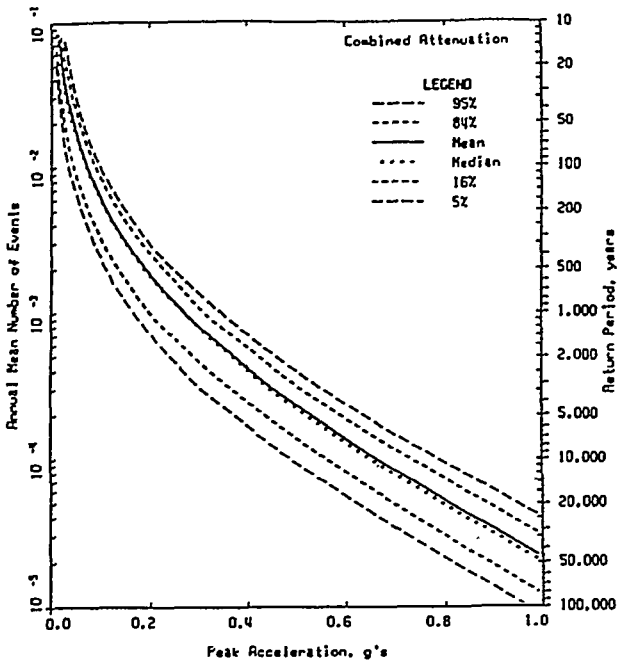

Figure 1. Distribution of peak horizontal acceleration at the surface developed for the ESF seismic hazard analysis (Figure A-6 from reference 12). Legend refers to probabilities.

strain in the repository block are discussed in following sections.

ROCKFALL

Fraction of Containers Damaged by Rockfall

For TSPA-1993, we assumed a repository design that included backfilled emplacement drifts; however, more recent potential repository designs have not included backfill.[14] In unbackfilled drifts, rockfall can be enhanced by seismic activity or thermal-mechanical stresses. Debris from rockfall has three effects on long-term performance: (1) rocks covering a container add thermal insulation, increasing container temperature; (2) rocks contacting a container form capillary pathways for water, increasing container corrosion; and (3) large blocks falling on a container cause direct damage.

It has been calculated that the impact of a 12-metric-ton block approaches the safety limit for an intact waste container (reference 15, p. 6-189). Here we take the failure threshold to be 12 metric tons and estimate the probability of a rock that big falling on a container. We assume that rockfall occurs on uncorroded containers; however, because corroded containers would likely fail under lesser forces, this assumption should be reinvestigated.

To estimate the distribution of rock-block sizes, we used a modified (log-space) version of the Topopah Spring

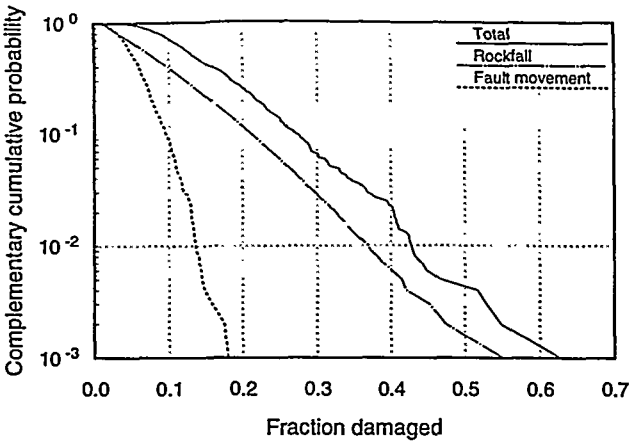

Figure 2. Distribution of the fraction of containers potentially damaged by rockfall and by fault displacement within one million years. (Some of these containers might fail by corrosion before being damaged by rockfall.)

fracture-spacing distribution developed for TSPA-1993 (reference 11, p. 7-28). The log-beta distribution has a large spread, with a mean of 0.7 m and a median of 0.2 m. To obtain block-mass distributions, cubic and parallelepiped blocks were considered, and the mean TSw bulk density (2258 kg/m^3) was used. Estimates of the fraction of containers likely to be hit by a 12,000-kg (or larger) block range from 2% to 55%, with the lower values considered to be most likely. For the Monte Carlo simulations, a beta probability distribution for the fraction of containers potentially damaged by rockfall is defined with a minimum of 1%, maximum of 100%, mean of 10%, and standard deviation of 8% (Figure 2). The peak probability density occurs at about 2%, corresponding to an estimate using parallelepiped blocks; the mean of 10% corresponds to cubic blocks.

Timing of Container Damage

Data for rockfall timing and rates are site, design, and event specific, and analyses are still preliminary; thus, we rely heavily on assumptions and probability distributions to describe these parameters. We expect that the tunnels will be stable at first because of engineered ground support. The ground support is not expected to last very long, however, because of corrosion and thermal-mechanical stresses. Heating could improve stability at early times due to thermal expansion of the rock around the opening. As the rock cools off, we expect that the mechanically weakened tunnel walls and ceiling will collapse—either bit by bit or possibly all at once. The distribution of damage times used in this analysis (Figure 3) is calculated using the following assumptions.

- *Rockfall initiation.* The effect of temperature and seismicity on drift stability has been examined in several previous studies,[16,17] but uncertainty still exists concerning

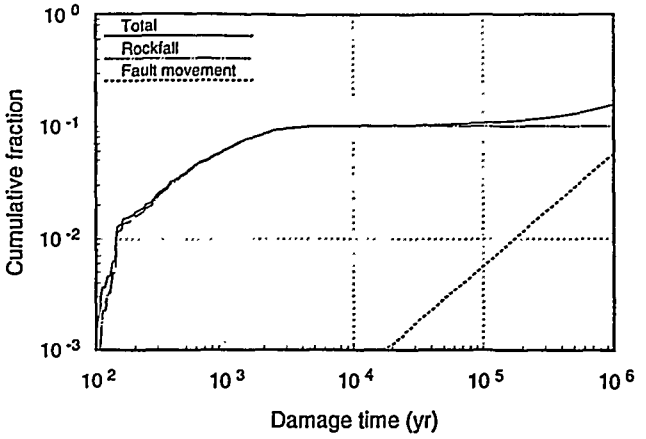

Figure 3. Mean distribution of the time at which containers are potentially damaged by rockfall and by fault displacement (some containers might fail by corrosion first). The rockfall distribution includes both rockfall due to thermal-mechanical stresses and earthquakes.

start times and rates of rockfall. For repository conditions as modeled for this analysis, the container and drift-wall temperatures peak within 100 yr; waste containers remain above boiling for 800 to 2000 yr. Although thermal expansion should add stability to the drift, we assume that rockfall onto containers will start sometime between 100 yr and 2000 yr after emplacement. A uniform probability distribution is used for sampling (to maximize uncertainty).

Rockfall rate. Convergence rates have been measured for a tunnel in welded tuff at the Nevada Test Site,[18] ranging from 0.001 to 0.006 mm/day. At 0.001 mm/day, a 4.3-m emplacement drift would close in about 12,000 yr. The convergence rate is expected to decline with time, so this estimate might be low. On the other hand, thermal effects could accelerate the convergence in an emplacement drift. We simply round up to 15,000 yr for the maximum period during which rockfall damage might occur. The minimum of the rockfall-damage period is taken to be 1 yr, representing the possibility of collapse of all the drifts in the repository at the same time (collapse of subsequent drifts possibly being triggered by collapse of the first one). In the absence of any better information, a uniform distribution between the minimum and maximum (again maximizing uncertainty) is used for sampling. The rate of rockfall damage to containers is also taken to be uniform during the rockfall-damage period.

Seismically induced rockfall. Rockfall failures are coupled to the seismic-events model by the assumption that a major earthquake can cause tunnel collapse (Jung *et al.*[17] show, with caveats, 0.4*g* collapsing a drift). In this analysis, if an earthquake above the threshold (see above) occurs after 100 yr and before the end of the rockfall-damage period, any remaining rockfall damage is taken to occur at that time. For example, if in a given realization it is sampled that some number of the containers are to fail because of rockfall and an earthquake above the damage threshold occurs at a time when 10% of those containers have failed, the other 90% are assumed to fail at the time of the earthquake.

Moisture Contact With Waste Containers

This subsection applies only to the composite-porosity model. In TSPA-1993, it was shown that the fraction of containers in contact with rubble was an important model parameter for the composite-porosity model because of the assumption that rubble contact provides moisture contact and therefore promotes aqueous corrosion when temperatures are below boiling (reference 11, p. 14-64). Recent unpublished work (personal communication by T. A. Buscheck and reference 19) has indicated that backfill may actually reduce aqueous corrosion by lowering the relative humidity near the waste packages. For this analysis, we retain the corrosion and water-contact models used in TSPA-1993 and so the humidity effect is not included. Future work should examine the impact of relative humidity on the results.

We assume that rubble contact starts at the same time that rockfall damage starts (between 100 yr and 2000 yr after waste emplacement, as discussed above), and that the fraction of containers with rubble contact ramps up linearly to 1 over some period of time. The time period for initiation of rubble contact should be less than the time period for rockfall damage, because rubble contact only requires a relatively small amount of rubble, whereas there is potential for rockfall damage until the waste packages are completely covered by rubble.

For one possible emplacement geometry (drift diameter 4.3 m, container diameter 1.75 m, liner thickness 0.1 m, invert height 0.5 m, and pedestal height 0.15 m), rubble contact only takes 17% as much fill material as is needed to completely cover the container. Seventeen percent of 15,000 gives 2500, so we vary the rubble-contact-initiation period between 1 yr and 2500 yr. Rather than take the rubble-contact-initiation period to be a fixed fraction of the rockfall-damage period, the two are sampled separately but a rank correlation of 0.9 is applied so that small rubble-contact-initiation periods go with small rockfall-damage periods and large rubble-contact-initiation periods go with large rockfall-damage periods.

As with container damage, rubble contact is coupled with the seismic-events model by increasing the rubble-contact fraction f_r all the way to 1 if there is an above-threshold earthquake before f_r would otherwise have reached 1.

Temperature Increase Caused by Rockfall

We expect that rockfall rubble will act as a thermal blanket the same way that backfill does, and the resultant temperature rise could be important. To get temperature histories for the Monte Carlo simulations, in which the time and duration of rockfall are variable, we interpolate between the TSPA-1993 temperature curves,[11] which include backfilling 75 yr after waste emplacement, and temperature curves resulting from no backfill.

Analysis of the TSPA-1993 temperature curves shows that the near-field temperature is quasi-steady state, and the difference between container temperature with and without backfill is proportional to the heat-generation rate: $\Delta T(t) \propto Q(t)$. This result implies that the container-temperature curve for backfilling at 200 yr, for example, can be obtained by following the "no-backfill" temperature curve until $t = 200$ yr and then jumping up to the "backfill" temperature curve. An additional complication is that the thermal properties (thermal conductivity, in particular) of crushed-tuff backfill are not well known,[20] and the thermal properties of rockfall rubble even less so. Analyses of recent backfill heater tests[20,21] show an effective thermal conductivity of 0.58–0.74 W/mK, whereas the TSPA-1993 calculations assumed a thermal conductivity of 0.2 W/mK. For an idealized problem with axial symmetry the temperature solution can be found analytically,[19] and the difference between container temperature with and without backfill, ΔT, is inversely proportional to the backfill thermal conductivity. Thus, a thermal conductivity a factor of 3 higher would imply a temperature increase a factor of 3 smaller (on the order of 100°C rather than 300°C).

Rockfall rubble will presumably be much less uniform and less well characterized than an engineered backfill. The thermal conductivity of the rockfall rubble is a function of the effective porosity (higher porosity implies lower conductivity), plus shape factors.[20] The porosity and particle-size distribution for rockfall rubble are not known, but random blocks falling from the ceiling would probably result in a higher porosity than backfilling with small, relatively uniform-size crushed tuff.

To cover the uncertainties given above, a range of 0.2 W/mK to 0.75 W/mK is used for rubble thermal conductivity κ_b. The temperature difference ΔT calculated for TSPA-1993 is then scaled by the ratio $0.2/\kappa_b$ to produce the temperature difference used in this analysis.

The timing of the change from "no backfill" temperature to "backfill" temperature is handled in the same way as for rockfall container damage. We assume that the temperature curves ramp up linearly from the "no backfill" curve to the "backfill" curve (with the appropriate conductivity scaling) over the rockfall-damage time period. And, as before, the ramp-up time is adjusted if there is a large enough earthquake that causes earlier rockfall. Note that in reality the ramp-up between the two temperature regimes is nonlinear.

FAULT DISPLACEMENT

Determination of fault displacement and changes in strain within the potential repository block requires an estimate of the magnitude of the seismic event. Based on the relationship between seismic acceleration and distance given in Figure A-9 of reference 12, we estimate a standard deviation of a distribution (assumed to be normal) of hypocentral distances from the repository for a given acceleration. We then randomly sample a distance and estimate the local magnitude, M_L, using an attenuation relationship from McGarr *et al.*[22] (The resulting magnitude distributions closely resemble those shown in the referenced figure.) Because a potential repository would be located relatively near the surface compared with the depths being considered, we assume that only earthquakes capable of causing surface rupture would cause fault displacement in the repository block. The lower bound for such earthquakes is randomly selected between M_L 6 and 6.5.[12,23]

Once the magnitude is known, we use empirical data[9] to estimate several quantities: the length of the rupture on the primary fault (for a given event, we define the primary fault as the one whose displacement generates the release of the most energy); the offset of the primary fault; and the width of the zone where secondary faulting occurs. The data used include both normal-slip and strike-slip earthquakes. Linear regressions are made of the quantities of interest with respect to magnitude. For a given magnitude, the rupture length, offset, and secondary-faulting zone are calculated directly (i.e., without uncertainty).

Knowing the above quantities, we can probabilistically determine whether a fault intersects the repository. Using the hypocentral distance and the depth, which is randomly sampled between 3 km and 15 km,[12] the epicenter of the event is located at a point in space. Using the rupture length (assuming that the hypocenter corresponds to the center of the rupture) and a randomly sampled orientation, a trace representing the rupture on the primary fault is determined. Using the width of the secondary-faulting zone, a rectangular area is constructed around the trace (assuming that the trace is in the center of the secondary-faulting zone). We approximate the repository with a simple circular geometry to determine whether the repository is intersected by either (1) the primary trace, or (2) the secondary-faulting area. (Circular geometry allows absolute orientation of the primary fault and centering of the primary fault in the secondary-faulting zone to be unimportant; however, it does introduce error. Most existing faults trend north-northeast in the area. Future work should incorporate the actual geometry of known faults.)

If the primary trace intersects the repository, then fault displacement occurs in the repository and the number of containers that could be damaged is calculated. For simplicity, we assume that secondary faults do not intersect the repository if the primary fault does. If the primary trace misses the repository but the secondary-faulting area intersects it, we estimate by random choice whether fault displacement actually occurs in the repository. This randomness allows us to determine the sensitivity of the results (the releases of radionuclides) to secondary faulting.

The number of damaged containers is calculated by drawing the trace through the repository area and estimating how many containers would be contacted. We assume that the containers are uniformly distributed, that faulting occurs at unknown locations (either faults are not avoided or do not yet exist during emplacement), and that all contacted containers fail. This model typically predicts fault displacement in the repository to occur about every 30,000 to 50,000 yr, and about 20 containers are damaged for each occurrence (see Figures 2 and 3).

FLOW-PATH CHANGES

Redistribution of strain within Yucca Mountain, opening some fractures or faults and closing others, is considered as a mechanism to change flow patterns and fluxes. Thermal effects of the repository might also induce strain changes, similar in scale to seismic events, that could cause pathway changes. In addition, other important seismically induced hydrologic changes could occur; e.g., changes to perched-water systems, groundwater infiltration, and flow directions in the saturated zone. Here we consider only changes in fracture-flow patterns in the unsaturated zone induced by seismic activity.

Assuming normal faulting, the region around a fault displaced 1 m ($M_L \approx 6.5$) that would undergo a change of greater than 10 microstrain (i.e., a change in volume of 10×10^{-6}) is approximately circular, ignoring small zones of tension at the ends of the rupture, with the rupture length being the diameter of the circle (Figure 4—the model used to create the figure is discussed in the next section). The choice of 10 microstrain is arbitrary; it implies a reduction of 10 μm in 1 m, or potentially the closing of a 100 μm fracture every 10 m. Again using circular geometry, the part of the repository that would see a change in strain, and therefore perhaps a change in flow pattern, is calculated as the intersection of two circles, one approximating the repository, the other approximating the strain area. Typically, some part of the repository is predicted to see a change in strain every few thousand years.

The strain-change fraction is used by the weeps model to determine the number of flow paths that change locations for a given seismic event. The actual number of flow paths relocated is randomly selected (between none and the total in the strain region), again to allow estimation of the sensitivity of the results to this effect. In general, changing flow patterns should reduce the time that weeps contact specific containers, resulting in fewer corrosion failures and thus fewer releases from corrosion-failed containers. Conversely, if weep flow is continually being redirected, there is a greater probability of contacting mechanically damaged containers, resulting in more releases from them.

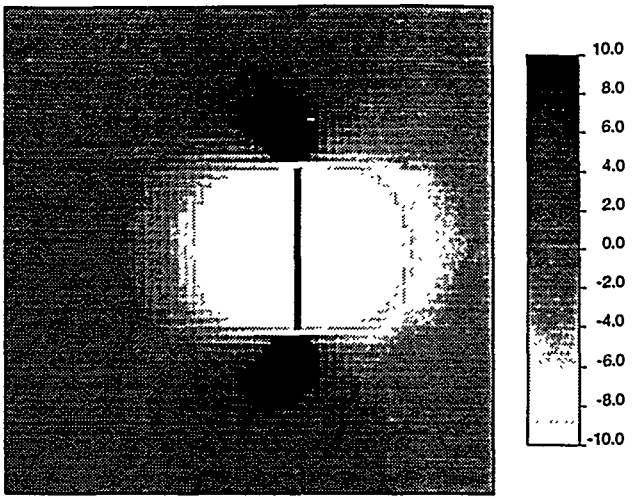

Figure 4. Map view of changes in strain calculated for a 10-km rupture displaced 1 m along a normal fault dipping 60° W. Area depicted is 30 km by 30 km. Scale shows volumetric strain (times 10^6). Light areas indicate compression; dark areas indicate tension.

WATER-TABLE RISE

Earthquakes have been observed to cause strain-induced changes in water-table elevation.[24] As part of this analysis, a series of calculations was conducted to re-examine the impact of seismic pumping on the water table. Unlike previous work,[25,26] these calculations were performed using a dual-permeability model. Because most seismically induced flow is expected to occur rapidly up fractures, a dual-continuum formulation is expected to provide a better approximation of the system response.

The faults that have been active most recently appear to be dominantly high-angle oblique-slip;[4] no low-angle movement has been recorded, although detachment faults have been observed in the vicinity. However, in order to investigate the sensitivity of co-seismic water-table response to fault-displacement type, three different fault types were considered: (1) dip-slip displacement to a depth of 10 km along a normal fault dipping 60°; (2) dip-slip displacement to a depth of 2 km along a listric fault dipping 5°; and (3) right-lateral strike-slip displacement along a fault dipping 60°. For all three types, a 1-m displacement with a rupture

length of 30 km was considered, corresponding nominally to a 6.5 M_L earthquake.

Distribution of strain was calculated using a three-dimensional elastic boundary-element model (Figure 5).[27] Poroelastic coupling between the tectonics model and the groundwater flow model (TOUGH2) was implemented using strain sensitivities (the proportionality between strain and pore pressure) estimated for the saturated volcanic section and underlying carbonate aquifer.[28] The change in pressure resulting from the strain was added to the steady-state solution of the flow model to determine the initial conditions for the transient problem.

Results indicate that the greatest response of the water table occurs for the stike-slip scenario: complete saturation in the fractures occurs within 1 hr to an elevation of 50 m above the steady-state water table directly above the fault. However, fracture saturation drops to less than 10% within 20 hr. At 10 m above the water table, saturated conditions persist over a large area of the hanging wall for 500 hr. Matrix saturations change little. Steady-state conditions return within 6 mo. For comparison, estimates of water-table rise during past climates range from 80 m to 115 m.[29]

The calculated water-table rise is insufficient to inundate a repository, even considering an elevated water table during a wetter climate. The calculated rise also does not encroach upon the thermal dry-out regions calculated for TSPA-1993 (at least not for a dry climate; the thermal dry-out region during a wet climate was not calculated). In general, seismically induced water-table excursions caused by poroelastic coupling would not influence the models presently being used to determine long-term performance of a repository at Yucca Mountain; therefore, we excluded them from the total-system simulations.

TOTAL-SYSTEM SIMULATIONS

TSPA-1993 Background

In order to assess the effects of seismic activity on total-system performance, we tested our models using TSPA-1993[11] as a starting point. Processes included in the TSPA-1993 models were aqueous and gaseous flow and transport, climate changes, conductive heat transport, container wetting and corrosion, "protection" of containers by thermal dryout, "shedding" of thermally displaced water, fuel alteration and dissolution, human intrusion by exploratory drilling, and basaltic igneous intrusion. In this analysis, we do not consider human intrusion or igneous intrusion—only aqueous and gaseous releases. We use the 57-kW/acre, in-drift-emplacement case from TSPA-1993 as the baseline for this analysis, except we assume that the drifts are not backfilled.

A major result of TSPA-1993 was that repository performance is sensitive to the model of flow assumed in the

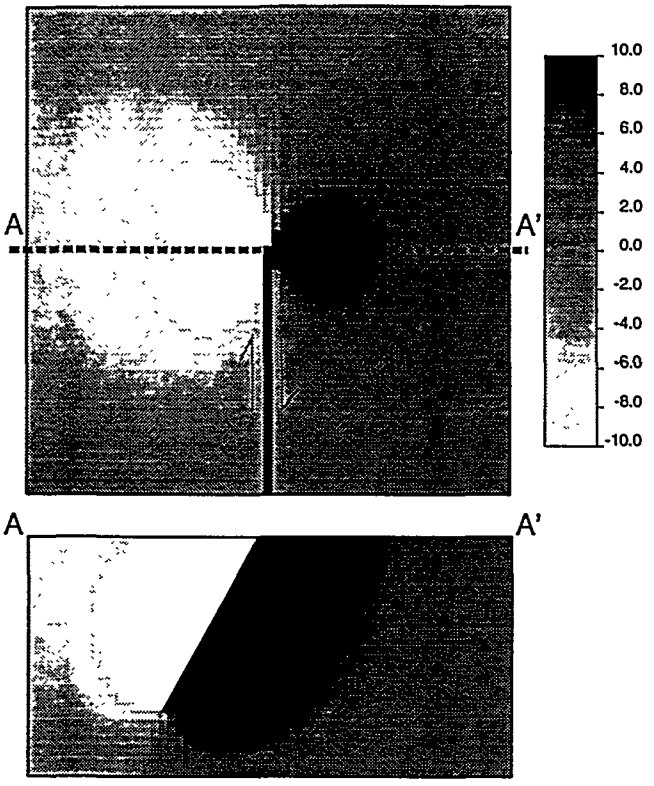

Figure 5. Map and profile views of the calculated strain resulting from strike-slip fault displacement. Upper area is 30 km by 30 km, lower area is 30-km long by 15-km deep. Scale shows volumetric strain (times 10^6). Light areas indicate compression; dark areas indicate tension.

unsaturated zone at Yucca Mountain. In the composite-porosity model, matrix and fracture flow and transport were strongly coupled; in the weeps model, they were completely uncoupled, with flow and transport occuring only in fractures. Release results differed primarily because of differences in wetting of waste containers. In the composite-porosity model, flow was taken to be relatively uniform: most containers were contacted by water, failed due to aqueous corrosion, and released their radionuclides to the geosphere, where they travelled relatively slowly to the accessible environment. In the weeps model, water was assumed to travel instantaneously through the unsaturated zone through fractures. However, most containers were never contacted by water, so only a small fraction failed due to aqueous corrosion and released radionuclides.

The TSPA-1993 calculations contained a number of assumptions and limitations, and the same assumptions and limitations apply to this analysis.

Results of the Composite-Porosity Model

The results for the composite-porosity model are shown in Figures 6 through 9. Each figure shows curves

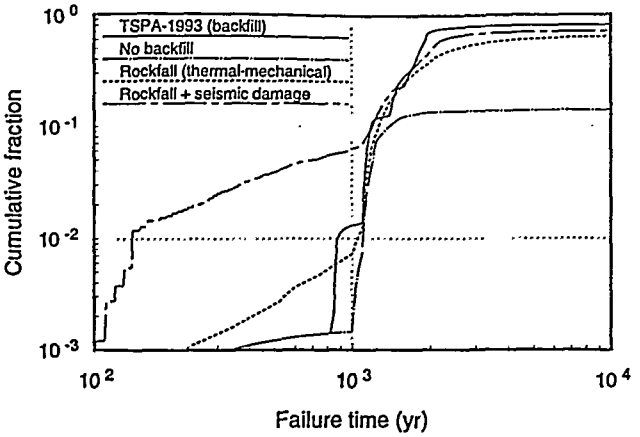

Figure 6. Mean container-failure distributions for the composite-porosity model.

from four simulations for comparison. The simulations are as follows.

- The "TSPA-1993 (backfill)" curve shows the results from TSPA-1993 for a backfilled repository.
- The "No backfill" simulation is just like TSPA-1993 except that the drifts are not backfilled. The rubble-contact fraction f_r is set to 0 instead of 1, and the temperature curves do not include the increase in temperature caused by backfilling.
- The "Rockfall (thermal-mechanical)" simulation is similar to the "No backfill" simulation except that rockfall effects due to thermal-mechanical stresses are included.
- The final results for this study are labelled "Rockfall + seismic damage," and include rockfall effects due to thermal-mechanical stresses and earthquakes and damage due to fault displacement within the repository block.

Note that only Column 8 was used in the aqueous-release calculations. The composite-porosity aqueous-release simulations for TSPA-1993 divided the repository into eight columns and added the releases from all columns to obtain the total releases, but one column is sufficient to see the effects of the processes of interest for this study.

In each of the figures, the "No backfill" curve is significantly different from the others. Additional analyses not shown indicate that the primary cause of the difference is the difference in rubble-contact fraction rather than the difference in temperature. This result points out the importance of assumptions about container wetting within the corrosion models (rubble contact is assumed to allow moisture to contact the waste containers).

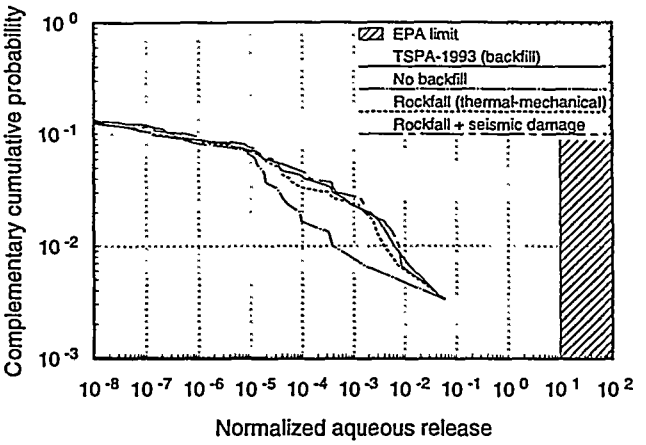

Figure 7. Distributions of 10,000-yr normalized cumulative aqueous release for the composite-porosity model (Column 8 only).

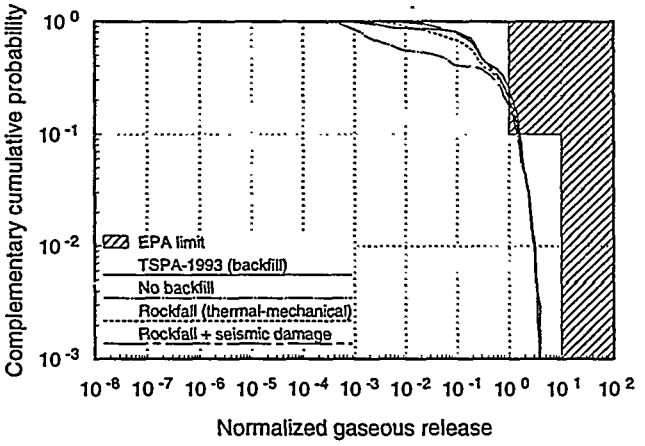

Figure 8. Distributions of 10,000-yr normalized cumulative gaseous release for the composite-porosity model.

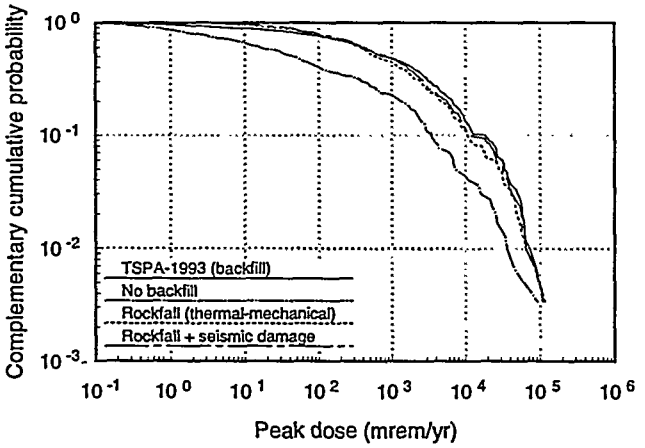

Figure 9. Distributions of peak individual drinking-water dose over 1,000,000 yr for the composite-porosity model (Column 8 only).

Figure 6 shows that our assumptions about seismically induced rockfall lead to a significant increase in the number of containers that fail early (before 1000 yr), but Figures 7 through 9 show that those early failures do not translate into significant increases in 10,000-yr releases or million-year doses. The reason for the lack of impact on releases is that most of the containers that fail early would fail before 2000 yr anyway—still well before 10,000 yr. Thus, the early failures caused by earthquakes might be significant in terms of the Nuclear Regulatory Commission's "substantially complete containment" requirement, but have little significance in terms of total-system releases.

Figures 7 through 9 show that inclusion of rockfall and fault-displacement effects do not significantly change calculated releases from those calculated for TSPA-1993. For the models used, it can be seen that there would be a significant reduction in releases if drifts are not backfilled and no rockfall occurs, but we do not expect the drifts to remain stable and intact over long periods of time. In the final simulation that includes models for rockfall and seismic effects, none of the rockfall or seismic parameters has a significant correlation with the calculated releases or doses. Linear regression analysis indicates the same parameters to be important as in TSPA-1993 (reference 11, Section 14.6.3)—primarily parameters having to do with water flow and container wetting.

Results of the Weeps Model

Figures 10 through 12 present the results of the weeps-model calculations. The cases shown in the figures are similar to those discussed for the composite-porosity model, except that the "Rockfall + seismic damage" case includes changes in flow patterns caused by seismically induced changes in strain.

Gaseous releases are produced by the weeps model when containers fail; aqueous releases are produced only when weeps contact failed containers. Unlike the composite-porosity model, the weeps model typically predicts very few (~0.1%) corrosion-failed containers, because few containers are contacted by weeps when they are warm and susceptible to corrosion. And again unlike the composite-porosity model, in the weeps model the geosphere poses little barrier to radionuclides once they are released. Thus, the weeps model discriminates between cases with few mechanical failures (the juvenile failures in the "TSPA-1993" and "No backfill" cases) and the cases with many mechanical failures (the "Rockfall (thermal-mechanical)" and "Rockfall + seismic damage" cases). In the worst realizations, however, when high groundwater fluxes and poor luck conspire to generate a large number of corrosion failures, corrosion failures dominate, as indicated by the confluence of curves at the greatest gaseous releases and doses.

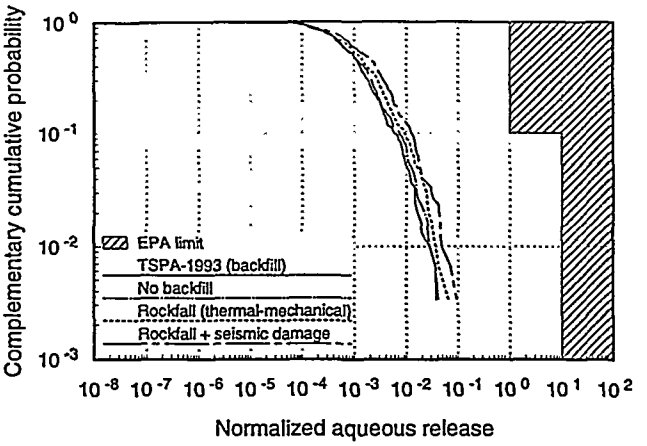

Figure 10. Distributions of 10,000-yr normalized cumulative aqueous release for the weeps model.

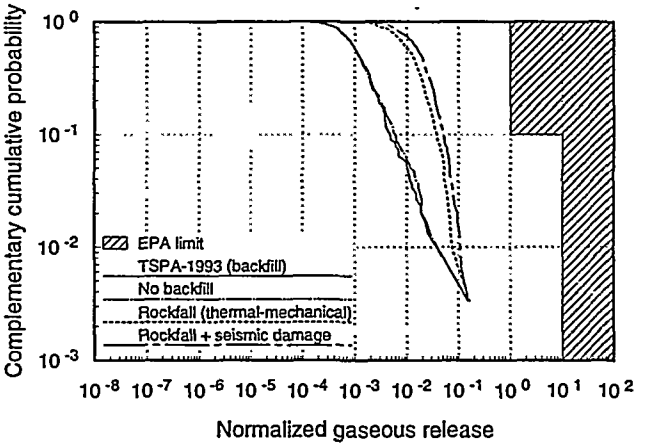

Figure 11. Distributions of 10,000-yr normalized cumulative gaseous release for the weeps model.

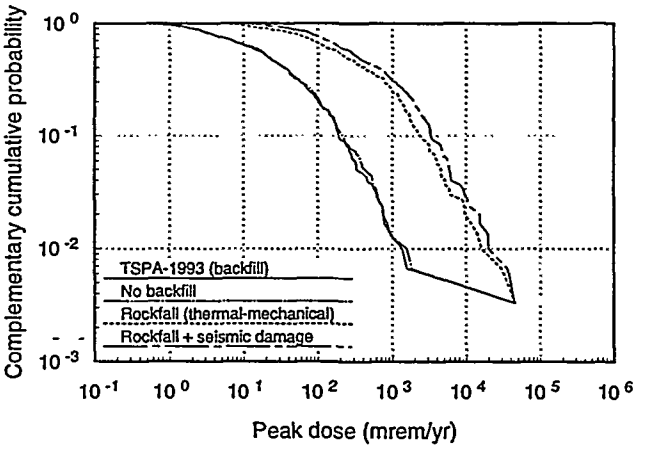

Figure 12. Distributions of peak individual drinking-water dose over 1,000,000 yr for the weeps model.

Figures 10 through 12 show that inclusion of rockfall and fault-displacement effects do affect calculated releases compared with TSPA-1993. Increased releases are especially significant at both early and late times: at early time, flow patterns are changing rapidly in response to the thermal pulse and weeps can contact containers near the time of failure; at late time, seismically induced changes in flow patterns allow weeps to contact previously failed containers. It is important to note, however, that most of the effect is caused by rockfall damage to containers, and rockfall can be mitigated by an appropriate repository design. In the simulation that includes models for rockfall and seismic effects, several rockfall and seismic parameters have a significant correlation with the calculated releases or doses. For TSPA-1993, linear regression analysis indicated that the important parameters related to water flow, climate change, corrosion rates, and geochemical retardation (reference 11, Section 15.5.4). From this analysis, we can add the following: (1) the fraction of containers damaged by rockfall; (2) the threshold value for seismic acceleration that would cause more than minor damage; (3) the timing of rockfall; and (4) the minimum earthquake magnitude necessary to cause surface rupture.

CONCLUSIONS AND OPEN ISSUES

If flow percolates through Yucca Mountain in a relatively slow, uniform manner, then seismic and rockfall effects should not have a significant impact on radionuclide releases. If flow moves rapidly in saturated pulses, then seismic events and especially rockfall could cause significant increases in radionuclide releases over long time periods. Backfilling in the repository could mitigate these effects. These conclusions are dependent on whether the total-system models used in this analysis reasonably describe the processes and events that determine the long-term performance of a repository at Yucca Mountain.

This analysis indicates additional data and further analyses that could better define the impact of seismic (and thermal-mechanical) effects on a potential repository. Data needs include the following: (1) the amount of rockfall and the size of the fallen rocks for given seismic accelerations and thermal loads; (2) changes in fracture/fault apertures for a given seismic perturbation, including surface changes that could influence infiltration and changes in permeability affecting perched water;[30] (3) the longevity of effective roof support; (4) the actual threshold value of seismic acceleration that could cause significant damage to drifts; and (5) characterization of secondary faulting in the region, including the probability of occurrence. Suggested future analyses are as follows: (1) detailed thermal-mechanical modeling, concentrating on drift stability (with and without seismic accelerations) and thermal-induced faulting resulting from large-scale thermal expansion;[17] (2) better modeling of container puncture by rockfall; (3) modeling of container damage by shaking during an earthquake; and (4) changes in hydrology caused by seismicity, including changes to perched water, groundwater infiltration, saturated-zone flow paths, and transmissivity in the saturated zone that could cause relatively permenant changes in the water table. Because backfill could be protective against rockfall, it is also suggested that the thermal, hydrologic, and mechanical properties of backfill be determined.

ACKNOWLEDGMENTS

This work was performed under the auspices of the U. S. Department of Energy, Office of Civilian Radioactive Waste Management, Yucca Mountain Site Characterization Office, under Contract DE-AC04-94AL85000. The work was performed under YMP WBS number 1.2.5.4.1, and was governed by work agreement WA-0172 Rev. 00. The input data used in this paper may not be QA qualified; the output data that are presented are not QA qualified.

REFERENCES

1. U. S. Department of Energy, *Site Characterization Plan, Yucca Mountain Site, Nevada Research and Development Area, Nevada*, DOE/RW-0199, U. S. Department of Energy, Washington, DC (1988).

2. J. L. Younker *et al.*, *Report of Early Site Suitability Evaluation of the Potential Repository Site at Yucca Mountain, Nevada*, SAIC-91/8000, Science Applications International Corporation, Las Vegas, NV (1992).

3. J. R. Park, R. G. Baca, N. A. Eisenberg, R. W. Janetzke, and B. Sagar, "IPA Phase 2 Total System Code and Scenario Analysis," in *Proceedings of the Fifth Annual International Conference on High Level Radioactive Waste Management*, 1461–1468, American Nuclear Society, La Grange Park, IL (1994).

4. A. M. Rogers, S. C. Harmsen, and M. E. Meremonte, *Evaluation of the Seismicity of the Southern Great Basin and its Relationship to the Tectonic Framework of the Region*, USGS-OFR-87-408, U. S. Geological Survey, Denver, CO (1987).

5. K. F. Fox Jr. and M. D. Carr, "Neotectonics and Volcanism at Yucca Mountain and Vicinity, Nevada," *Radioactive Waste Management and the Nuclear Fuel Cycle*, 13, 37–50 (1989).

6. R. B. Scott, "Tectonic Setting of Yucca Mountain, Southwest Nevada," in *Basin and Range Extensional Tectonics Near the Latitude of Las Vegas, Nevada*, edited by B. P. Wernicke, GSA Memoir 176, 251–282, Geological Society of America, Boulder, CO (1990).

7. B Crowe, F. Perry, *et al.*, *Status of Volcanism Studies for the Yucca Mountain Site Characterization Project*, LA-12908-MS, Los Alamos National Laboratory, Los Alamos, NM (1995).

8. R. W. Barnard, M. L. Wilson, H. A. Dockery, J. H. Gauthier, *et al.*, *TSPA 1991: An Initial Total-System Performance Assessment for Yucca Mountain*, SAND91-2795, Sandia National Laboratories, Albuquerque, NM (1992).

9. R. K. McGuire *et al.*, *Demonstration of a Risk-Based Approach to High-Level Waste Repository Evaluation: Phase 2*, EPRI TR-100384, Electric Power Research Institute, Palo Alto, CA (1992).

10. P. W. Eslinger *et al.*, *Preliminary Total-System Analysis of a Potential High-Level Nuclear Waste Repository at Yucca Mountain*, PNL-8444, Pacific Northwest Laboratory, Richland, WA (1993).

11. M. L. Wilson, J. H. Gauthier, R. W. Barnard, *et al.*, *Total-System Performance Assessment for Yucca Mountain—SNL Second Iteration (TSPA-1993)*, SAND93-2675, Sandia National Laboratories, Albuquerque, NM (1994).

12. CRWMS M&O, *Seismic Design Inputs for the Exploratory Studies Facility at Yucca Mountain*, Document No. BAB000000-01717-5705-00001 Rev. 00, TRW Environmental Safety Systems Inc., Las Vegas, NV (1994).

13. C. H. Dowding and A. Rozen, "Damage to Rock Tunnels from Earthquake Shaking," *Journal of the Geotechnical Engineering Division, Proceedings of the American Society of Civil Engineers*, **104**, 175–191 (1978).

14. CRWMS M&O, *Controlled Design Assumption Document (CDA)*, Document No. B00000000-01717-4600-00032 Rev. 00A, TRW Environmental Safety Systems Inc., Las Vegas, NV (1994).

15. CRWMS M&O, *Initial Summary Report for Repository/Waste Package Advanced Conceptual Design*, Document No. B00000000-01717-5705-00015 Rev. 00, TRW Environmental Safety Systems Inc., Las Vegas, NV (1994).

16. M. P. Hardy and S. J. Bauer, *Drift Design Methodology and Preliminary Application for the Yucca Mountain Site Characterization Project*, SAND89-0837, Sandia National Laboratories, Albuquerque, NM (1991).

17. J. Jung, E. E. Ryder, E. A. Boucheron, E. Dunn, J. F. Holland, and J. D. Miller, *Design Support Analyses: North Ramp Design Package 2C*, TDIF 302273, DTN: SNT01122093001.001, Sandia National Laboratories, Albuquerque, NM (1993).

18. R. M. Zimmerman, R. A. Bellman Jr., and K. L. Mann, "Analysis of Drift Convergence Phenomena from G-Tunnel Welded Tuff Mining Evaluations," in *Proceedings of the 28th U.S. Symposium on Rock Mechanics*, 831–841, edited by I. W. Farmer *et al.*, A. A. Balkema, Boston, MA (1987).

19. J. C. Walton and P. C. Lichtner, "Quasi-Steady State Model for Coupled Liquid, Vapor, and Heat Transport," submitted to *Water Resources Research* (1995).

20. E. E. Ryder, R. E. Finley, J. T. George, C. K. Ho, R. S. Longenbaugh, and J. R. Connolly, *Bench-Scale Experimental Determination of the Thermal Diffusivity of Crushed Tuff*, SAND94-2320, in review (1995).

21. C. K. Ho and R. R. Eaton, *Studies of Thermohydrologic Flow Processes Using TOUGH2*, SAND94-2011, Chapter 3, Sandia National Laboratories, Albuquerque, NM (1994).

22. A. McGarr, R. W. E. Green, and S. M. Spottiswoode, "Strong Ground Motion of Mine Tremors: Some Implications for Near-Source Ground Motion Parameters," *Bulletin of the Seismological Society of America*, **71**, 295–319 (1981).

23. C. M. dePolo, J. W. Bell, and A. R. Ramelli, "Estimating Earthquake Sizes in the Basin and Range Province, Western North America: Perspectives Gained from Historical Earthquakes," in *Proceedings of the International Topical Meeting on High Level Radioactive Waste Management*, 117–123, American Nuclear Society, La Grange Park, IL (1990).

24. R. H. Sibson, "Earthquake Rupturing as a Mineralizing Agent in Hydrothermal Systems," *Geology*, **15**, 701–704 (1987).

25. C. R. Carrigan, G. C. P. King, G. E. Barr, and N. E. Bixler, "Potential for Water-Table Excursions Induced by Seismic Events at Yucca Mountain, Nevada," *Geology*, **19**, 1157–1160 (1991).

26. J. D. Bredehoeft, "Response of the Ground-Water System at Yucca Mountain to an Earthquake," in *Ground Water at Yucca Mountain: How High Can it Rise?*, 212–222, National Academy Press, Washington, DC (1992).

27. Y. Okada, "Internal Deformation Due to Shear and Tensile Faults in a Half Space," *Bulletin of the Seismological Society of America*, **82**, 1018–1040 (1992).

28. D. Galloway and S. A. Rojstaczer, "Analysis of the Frequency Response of Water Levels in Wells to Earth Tides and Atmospheric Loading" in *Proceedings of the 4th Canadian/American Conference on Hydrogeology*, edited by B. Hitchon and S. Bachu, 100–113, National Water Well Association, Dublin, OH (1988).

29. J. B. Paces, E. M. Taylor, and C. Bush, "Late Quaternary History and Uranium Isotopic Compositions of Ground Water Discharge Deposits, Crater Flat, Nevada," in *Proceedings of the Fourth Annual International Conference on High Level Radioactive Waste Management*, 1655–1662, American Nuclear Society, La Grange Park, IL (1993).

30. S. Rojstaczer and S. Wolf, "Permeability Changes Associated with Large Earthquakes: An Example from Loma Prieta, California," *Geology*, **20**, 211–214 (1992).

DISCLAIMER